THE PROTEIN SOCIETY

Crystal Structure of the Small GTPase Arl6/BBS3 from *Trypanosoma brucei*

Glyn R. Hemsworth,[1] Helen P. Price,[2] Deborah F. Smith,[2] and Keith S. Wilson[1]*

[1]Structural Biology Laboratory, Department of Chemistry, University of York, Heslington, York, United Kingdom
[2]Centre for Immunology and Infection, Department of Biology, University of York, Heslington, York, United Kingdom

Received 24 September 2012; Revised 12 November 2012; Accepted 12 November 2012
DOI: 10.1002/pro.2198
Published online 26 November 2012 proteinscience.org

Abstract: Arl6/BBS3 is a small GTPase, mutations in which are implicated in the human ciliopathy Bardet–Biedl Syndrome (BBS). Arl6 is proposed to facilitate the recruitment of a large protein complex known as the BBSome to the base of the primary cilium, mediating specific trafficking of molecules to this important sensory organelle. Orthologues of Arl6 and the BBSome core subunits have been identified in the genomes of trypanosomes. Flagellum function and motility are crucial to the survival of *Trypanosoma brucei*, the causative agent of human African sleeping sickness, in the human bloodstream stage of its lifecycle and so the function of the BBSome proteins in trypanosomes warrants further study. RNAi knockdown of *T. brucei* Arl6 (*Tb*Arl6) has recently been shown to result in shortening of the trypanosome flagellum. Here we present the crystal structure of *Tb*Arl6 with the bound non-hydrolysable GTP analog GppNp at 2.0 Å resolution and highlight important differences between the trypanosomal and human proteins. Analysis of the *Tb*Arl6 active site confirms that it lacks the key glutamine that activates the nucleophile during GTP hydrolysis in other small GTPases. Furthermore, the trypanosomal proteins are significantly shorter at their N-termini suggesting a different method of membrane insertion compared to humans. Finally, analysis of sequence conservation suggests two surface patches that may be important for protein–protein interactions. Our structural analysis thus provides the basis for future biochemical characterisation of this important family of small GTPases.

Keywords: *Trypanosoma brucei*; Arl6; BBS3; BBSome; flagellum

Introduction

The protozoan parasite *Trypanosoma brucei* causes human African sleeping sickness with 10,000 new cases annually resulting in massive morbidity and mortality in Africa.[1] In the host bloodstream, the *T. brucei* flagellum is required for cell division[2–4] and for rapid variant surface glycoprotein recycling, a critical immune evasion strategy for parasite survival.[5] To avoid opsonisation by human antibodies, the trypanosome flagellum beats to direct surface bound immune complexes toward the flagellar pocket where they are rapidly endocytosed, hiding the parasite from the human immune system. The flagellum is also crucial for survival in the tsetse fly vector as it provides motility to enable the parasite to migrate from the midgut to the salivary glands where the flagellum is used to attach the parasite to the epithelium.[6–8] These key roles have led to the proposal that perturbation of flagellar function may be a viable avenue for the development of new drug treatments.[9]

Bardet–Biedl Syndrome (BBS) is a human genetic disorder with symptoms that include retinal degeneration, obesity, renal abnormalities, mental retardation, polydactyly, and hypogenitalism.[10] Mutations in 16 genes, found only in ciliates and flagellates, have been shown to result in BBS, in which the observed defects are all caused by dysfunction of the primary cilium, a non-motile thin protuberance found in many cell types which acts as a signalling and sensory organelle.[11,12] Seven of these genes (*BBS1*, *2*, *4*, *5*, *7*, *8*, and *9*) encode

*Correspondence to: Keith S. Wilson, Structural Biology Laboratory, Department of Chemistry, University of York, York YO10 5DD, UK. E-mail: keith.wilson@york.ac.uk

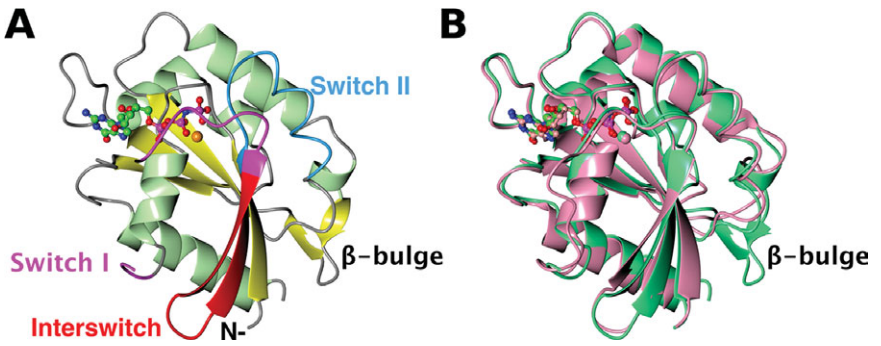

Figure 1. (A) The structure of *Tb*Arl6 coloured by secondary structure. The Switch I, Interswitch and Switch II regions are coloured magenta, red and blue respectively. The bound nucleotide analog is shown in ball and stick representation coloured by atom type and the Mg^{2+} ion as an orange sphere. (B) Human Arl6 (pink) superposed with *Tb*Arl6 (green). The β-bulge present in *Tb*Arl6 is the largest difference between the two protein structures. The structures in Figures 1–4 were produced with CCP4mg.[58]

proteins that form a large complex known as the BBSome, together with a protein of unknown function, BBIP10.[13,14] The BBSome is required for trafficking proteins to and from the primary cilium as shown in *BBS2* and *BBS4* knockout mice, which have defects in the trafficking of specific G-protein coupled receptors.[15,16] Recent data from a *Caenorhabditis elegans* model suggests that the BBSome interacts directly with intraflagellar transport (IFT) components and regulates IFT particle assembly.[17] How the BBSome does this remains uncertain, the current proposal being that it forms a coat complex for generation of vesicles to transport proteins to the base of the cilium.[18] Examination of kinetoplastid genomes, including those of the *Trypanosoma*, has revealed the presence of conserved orthologues of the BBSome subunits listed above. Given the consequences of BBSome mutations in humans, and since the flagellum plays such a crucial role in the survival of *T. brucei* within its host, analysing the structure and function of the BBSome from these parasites may be of fundamental importance to further elucidate the roles of this complex.

BBS3/Arl6 is a member of the ADP-ribosylation factor-like (Arl) family of small GTPases. Members of the Arf and Arl families are widely involved in regulating vesicle trafficking,[19] microtubule dynamics,[20] endosome-lysosome fusion,[21] and ciliogenesis.[22] They achieve these various functions by interacting with different protein partners, dependent upon their nucleotide bound state. While Arl6 is not a member of the core BBSome complex, mutations in the gene can cause BBS in humans.[23,24] These mutations result in either C-terminal truncations of the protein or changes in the highly conserved residues required for interaction with the guanine nucleotide.[25] Arl6 in its GTP bound state has been shown to assist in the recruitment of the BBSome to the base of the cilium.[18] Furthermore in a mouse model, Arl6 deletion resulted in BBS-like symptoms together with Arl6-specific phenotypes[26] whilst in *Caenorhabditis elegans* Arl6 was shown to undergo IFT.[27] In *T. brucei*, knockdown of Arl6 expression by RNAi resulted in a significant shortening of the flagellum although there was no loss of motility.[28] Genetic deletion of Arl6 could not be achieved, suggesting that it is essential for parasite viability. Furthermore, Price *et al.* [28] showed that the protein is *N*-myristoylated, interacts with tubulin and co-localises to the flagellar pocket with BBS1 when this protein is overexpressed, suggesting a functional association between *T. brucei* Arl6 and the BBSome as in humans.

Here we present the structure of *T. brucei* Arl6 (*Tb*Arl6) as a first step toward structure function studies of the BBSome from these parasites which provide excellent models for the study of cilium and flagellum function in eukaryotic cells.

Results

Structure of TbArl6

The 2.0 Å resolution structure shows a typical small GTPase with a single subunit in the asymmetric unit [Fig. 1(a) and Table I], consisting of a central 6-stranded β-sheet (residues 7–13, 43–50, 53–60, 79–85, 120–125, and 153–159) surrounded by six α-helices (residues 20–27, 92–103, 106–109, 135–142, 144–148, and 166–180). The similarity to other GTPases allows the definition of the switch I (residues 29–43), switch II (residues 59–72), and interswitch regions (residues 44–58) (Fig. 1), with a 3_{10} helix forming part of the switch II region. There is no electron density for four residues (32–35) in the switch I region, indicating their conformation is flexible. The central β-sheet consists largely of parallel strands apart from the third one which is antiparallel and forms part of the interswitch region, as seen in other members of the Arf and Arl family.[29] Five (15 including the His-tag) and nine residues are missing from the N- and C-termini respectively, presumed to reflect their intrinsic flexibility.

There was clear electron density for the GppNp non-hydrolysable substrate analog in a cleft on the

Table I. *Data Processing and Refinement Statistics*

Data processing	
Space group	$P3_221$
a, *b*, *c* (Å)	70.9, 70.9, 80.9
α, β, γ (°)	90.0, 90.0, 120.0
Radiation source	Diamond IO4
Wavelength (Å)	0.980
Resolution range (Å)	61.42–2.00 (2.11–2.00)
No. of observed reflections	168740 (26079)
No. of unique reflections	15861 (2373)
Completeness (%)	96.7 (100.0)
Multiplicity	10.6 (11.0)
$<I/\sigma(I)>$	15.0 (3.0)
R_{merge}	0.119 (0.839)
$R_{p.i.m.}$	0.038 (0.264)
Refinement	
Resolution range (Å)	61.42–2.00 (2.05–2.00)
No. of reflections (working/free sets)	15009/796 (1043/58)
Number of Atoms	1439
Final R_{work}	0.183 (0.229)
Final R_{free}	0.248 (0.235)
rmsd of bond lengths (Å)	0.010
rmsd of bond angles (°)	1.46
Overall average *B* factor (Å^2)	31.2
Ramachandran plot analysis	
Most favoured regions (%)	99.4
Additionally allowed regions (%)	0.6
Disallowed regions (%)	0.0

Values in the outer shell are given in parentheses.

surface of the protein (Fig. 2). This pocket is highly conserved amongst small GTPases and the interactions between protein and ligand are the same as in other structures. Fifteen direct hydrogen bonds are formed between the protein and GppNp with the specificity for GTP provided by the prototypical (N/T)KXD motif. The γ-phosphate forms a hydrogen bond to the main chain amide of Gly62 in the switch II region, an interaction that is important in inducing the active conformation of the protein. A single Mg^{2+} ion is coordinated by the Oγ's of Thr21 and Thr40 from the switch I region of the protein and by oxygen atoms from the β and γ phosphates of the ligand with the octahedral coordination sphere being completed by two water molecules.

Crystal contacts

Analysis of the structure using PISA[30] indicated that *Tb*Arl6 might form a dimer about the crystallographic two-fold with a buried surface area of 4460 Å^2 [Fig. 3(a)]. The interface involves 26 residues with four H-bonds and four salt bridges. Size Exclusion Chromatography with Multi-Angle Laser Light Scattering (SEC-MALLS) was used to analyse whether *Tb*Arl6 forms a dimer in solution. Samples were pre-incubated with 1 m*M* GppNp or 1 m*M* GDP and then applied to the SEC column. In the presence of GppNp, the major species had a molecular mass of 21.4 ± 1.3 kDa [Fig. 3(b)], and with GDP of 21.7 ± 1.5 kDa [Fig. 3(c)]. So, as the expected mass is 21803 Da, the protein is a monomer. A minor second peak was detected in both samples at a molecular mass of 53.1 ± 2.7 kDa in the presence of GppNp and 64.3 ± 3.9 kDa with GDP. We attribute these species to be the minor contaminant from the purification which was visible in SDS-PAGE.

Conserved regions in TbArl6

We constructed a model to look at sequence conservation on the protein surface with the aim of identifying possible surfaces with which protein partners might interact (Fig. 4). The four residues disordered in the switch I region were ordered in the human homologue and so this loop was added to the model in that conformation. Missing side chains were added in the most likely rotamers but the missing N- and C-termini were omitted as there was no reliable way of predicting their positions.

A BLAST search was used to identify Arl6 sequences from other species in Uniprot which were then aligned with *Tb*Arl6 using T-COFFEE.[31] To prevent the conservation being skewed by GTPases with other functions, only proteins annotated as Arl6 were included. The resulting alignment was

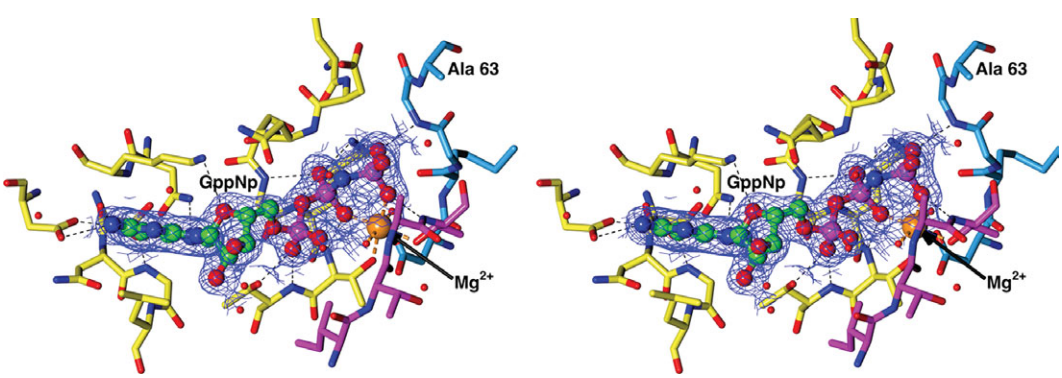

Figure 2. Stereo diagram of the electron density in the active site cleft contoured at 1σ. The residues which form the cleft are shown as sticks coloured by atom type with direct hydrogen bonds to the ligand shown as black dashed lines. Residues which form the switch I and II regions have magenta and blue carbon atoms respectively. Ala63, the residue, which is a Gln in most small GTPases and is important for the hydrolysis of GTP, is labeled.

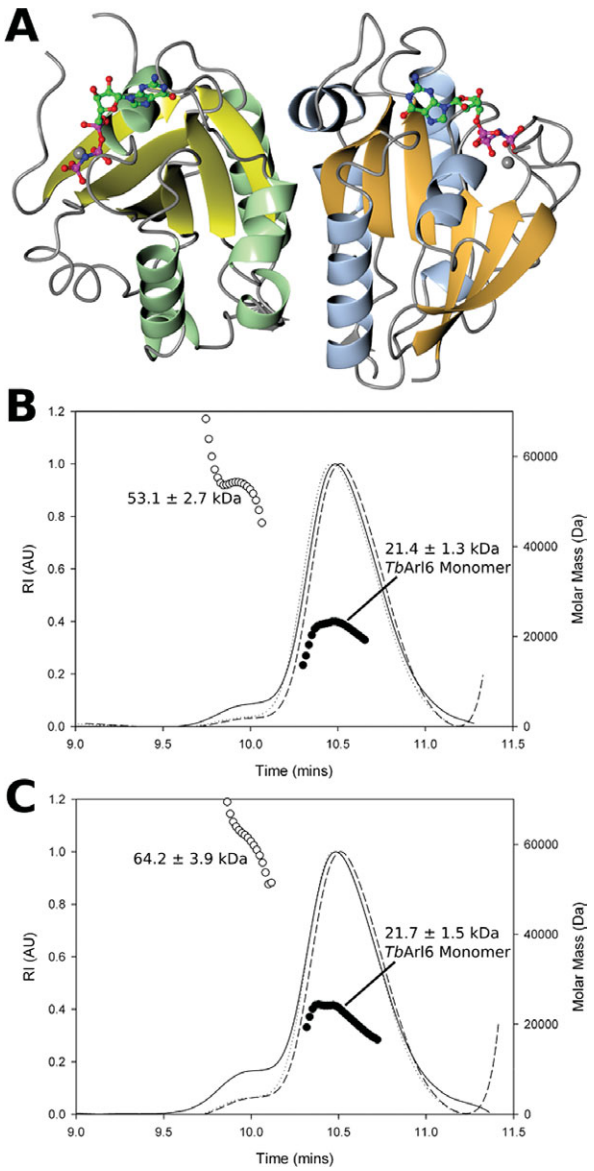

Figure 3. (A) Structure of the dimer suggested by PISA as an oligomeric assembly. (B) and (C) SEC-MALLS data in the presence of GppNp and GDP respectively indicating that *Tb*Arl6 at 5 mg/mL is a monomer in solution. The solid, dashed and dotted curves represent the Rayleigh ratio, UV light absorption, and differential refractive index respectively of the solution emerging from the SEC column. Open and closed circles represent the molecular mass of the species across the selected peaks calculated from the MALLS data.

uploaded to the ConSurf server to generate the sequence conservation scores on the protein structure.[32]

The use of Arl6-annotated sequences only, led to there being fewer sequences than is optimal for the analysis, which resulted in a lot of residues having insufficient data for scoring [Fig. 4(a,b)]. Nevertheless, the results show that the GTP binding pocket is highly conserved [Fig. 4(b)], as is an adjacent water filled cavity with a volume of 142 Å^3 [33] [Fig. 4(b)]. In addition, there are two much smaller clusters of conserved residues in two regions on the surface formed along the terminal strands of the central β-sheet and contributed to by the adjacent α-helices [Fig. 4(c,d)].

Discussion

Overall structure

Comparisons using secondary structure matching[34] show that the structure is very similar to that of human Arl6 (pdb code 2h57, RMSD of 1.14 Å over 163 Cα's corresponding to a sequence identity of 47%).[35] The largest difference is the presence of a β-bulge in *Tb*Arl6 due to a five residue insertion from residues 110 to 115 [Fig. 1(b)]. Hits were also obtained to other Arf and Arl structures in their activated state with GTP or non-hydrolysable ligand bound. *Tb*Arl6 is thus in its active conformation primed for interacting with its protein partners.

Crystal contacts

Analysis using PISA[30] indicated that *Tb*Arl6 might form a dimer [Fig. 3(a)]. Some GTPases are known to dimerise — Arf1 dimerisation, for example, is important for inducing membrane curvature to allow the formation of COPI vesicles.[36,37] Other small GTPases use dimerisation to regulate their activity, the dimerisation providing residues to aid in GTP hydrolysis.[38] However, the side-by-side topology for the dimer suggested by PISA is not indicative of this interaction playing a regulatory role. SEC-MALLS analysis conclusively showed *Tb*Arl6 to be a monomer in solution in the presence of either GppNp or GDP and we conclude that this is the probable biological unit. Nevertheless, dimerisation cannot be completely ruled out under other conditions, as with Arf1 dimerisation is only observed in the presence of membranes. The potential dimer in the crystal may hint at the possibility of a similar phenomenon for *Tb*Arl6.

The nucleotide binding pocket

The *Tb*Arl6 active site is typical of small GTPases but with one significant difference. There is a highly conserved glutamine residue (Gln73 in the human enzyme) in the active site of most small GTPases, proposed to be responsible for polarising or stabilising the nucleophilic water.[39,40] While Gln is substituted by His in some organisms, mutation to Ala is routinely used to produce a GTP locked form of the enzyme that has a greatly reduced ability to hydrolyse GTP.[41,42] In contrast, the natural residue at this position in *Tb*Arl6 is an alanine (Ala63), as noted by Price *et al.*[28] [Fig. 4(a)]. Since there is no obvious residue that could substitute for the role played by the Gln in activating the nucleophile (Fig. 2), *Tb*Arl6 is likely to have a reduced ability to hydrolyse GTP. In other small GTPases such as Ras-related proteins, the catalytic Gln is replaced by a threonine

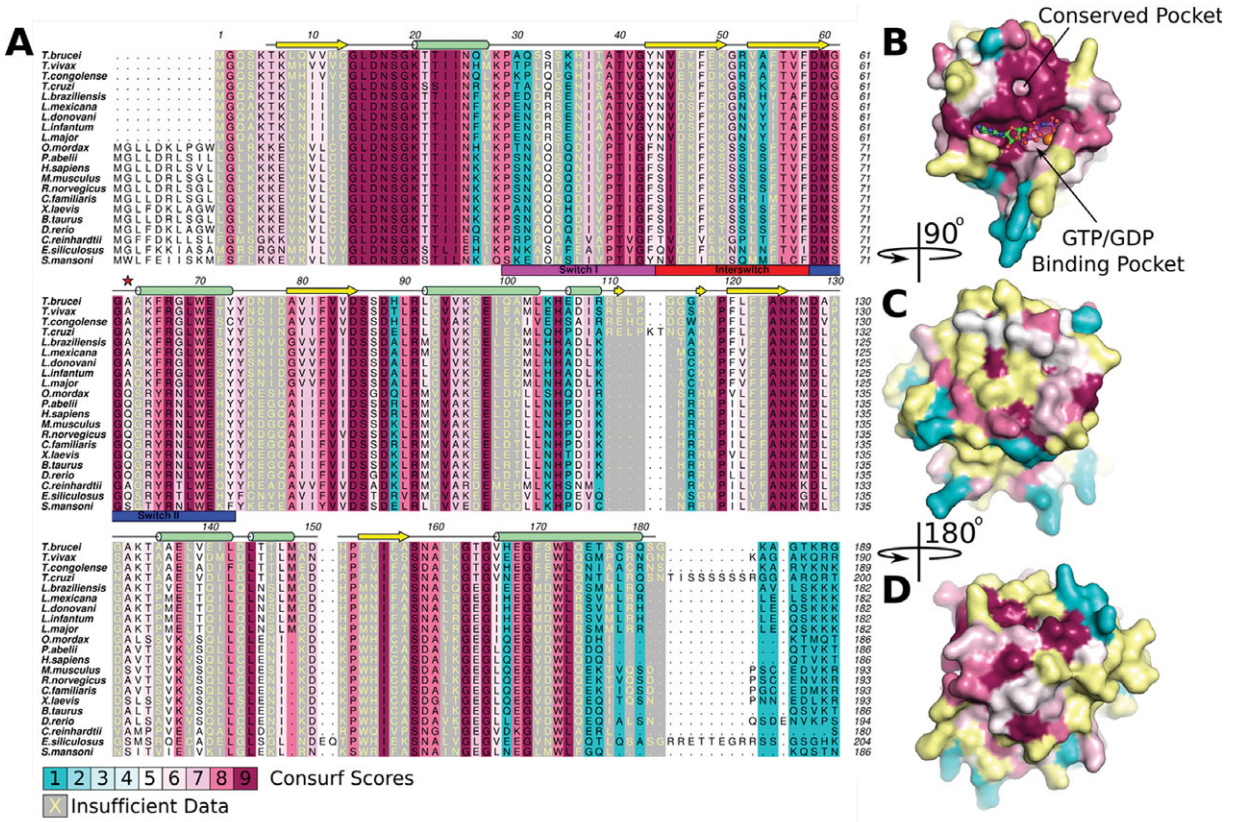

Figure 4. Consurf analysis for *Tb*Arl6. (A) Sequence alignment coloured by Consurf score according to the colour key shown. The secondary structure for *Tb*Arl6 is shown along the top of the alignment and Ala63 is indicated by the red star (Figure generated using ALINE[59]). (B–D) The sequence conservation on the *Tb*Arl6 surface. The GTPase pocket and an adjacent small pocket are both highly conserved (B) while the two surfaces at each end of the central β-sheet (C and D) also show some sequence conservation.

which interacts with a GTPase Activating Protein (GAP) partner.[43] This GAP provides an Asn "thumb" which acts as the catalytic residue inducing the GTPase activity.[44,45] *Tb*Arl6 may therefore require the action of a yet-to-be-identified GAP, a possibility which warrants further investigation.

Conserved regionsin TbArl6

We constructed a model to allow the analysis of sequence conservation on the protein surface to identify surfaces that Arl6 might use to interact with its protein partners. The region with the most sequence conservation was in and around the GTP binding site. Interestingly, adjacent to the GTP binding cleft is a conserved small water-filled pocket, also noted in previous Arf/Arl structures but with no proposals as to its function.[46,47]

There are two other conserved surfaces at each end of the central β-sheet which are contributed to by the adjacent α-helices. Price *et al*.[28] showed that *Tb*Arl6 interacts with tubulin and suggested that it links tubulin as a cargo to the BBSome in its proposed vesicle trafficking function. These surfaces may interact with tubulin and the BBSome bridging between them, but clearly much work is required to investigate this hypothesis further, especially as one of these surfaces is that which PISA suggests might represent a dimer interface.

The sequence alignment reveals significant differences in the N-termini of the trypanosomal proteins compared to their counterparts from higher eukaryotes [Fig. 4(a)]. The N-terminal portion of Arf/Arl proteins typically form an amphipathic helix which is tucked away on the protein surface and runs antiparallel to the C-terminal helix when GDP is bound but extends away from the protein to insert into and anchor the protein to membranes when GTP is bound.[48] Arfs are also *N*-myristoylated to further aid their interaction with membranes. The N-terminal helix is often truncated for crystallisation of Arf/Arl proteins, for example human Arl6.[35] While we crystallised the full-length protein, we could only model from residue six onwards, reflecting flexibility of these residues and suggesting that the shorter N-terminus for *Tb*Arl6 does not form a helix. The alignment in Figure 4(a) shows that the Arl6s from trypanosomes are all 10 residues shorter at their N-termini and so all lack the amphipathic helix predicted for the proteins from higher eukaryotes [Fig. 4(a)]. Possible sites of *N*-myristoylation

can be predicted using the N-terminal sequence motif, G-[EDRKHPFYW]-x(2)-[STAGCNDEF]-[P].[49] The *T. brucei* protein is known to be *N*-myristoylated *in vivo*[28] and sequence analysis suggests that *Trypanosoma vivax* Arl6 is also highly likely to be *N*-myristoylated. While the prediction was less strong for other trypanosome species, it is conceivable that they all have *N*-myristoylated Arl6 proteins.[50] None of the Arl6s with the extended N-termini seem to be candidates for *N*-myristoylation suggesting that these proteins use a different method of membrane attachment and localisation compared to trypanosomal Arl6s.

Conclusions

The structure of *T. brucei* Arl6 in complex with the non-hydrolysable GTP analog GppNp reveals a typical Arl structure but with significant differences compared to orthologues from other organisms including humans. The recent work of Price and co-workers[28] suggests that *Tb*Arl6, and perhaps the BBSome, have functions relating to the flagellum, an organelle of key importance in the trypanosome life cycle. This is clearly an area that warrants further investigation and the structure presented here will help guide future biochemical investigations of this important small GTPase.

Materials and Methods

TbArl6 expression and purification

N-terminally His_6 tagged *Tb*Arl6 was expressed from the pET-YSBLLIC vector as described in Price *et al*.[28] Cells were resuspended in 5 volumes of Buffer A (50 m*M* HEPES pH 7.0, 0.5 M NaCl, 5 m*M* $MgCl_2$, 1 m*M* DTT, 30 m*M* imidazole) and lysed by sonication. Cell debris was removed by centrifugation at 18,000 rpm in a Sorval SS-34 rotor for 30 minutes. The supernatant was removed and applied to a 5 mL His-trap column equilibrated in Buffer A. After washing with 4 column volumes (CVs) of Buffer A, a gradient was applied from 0 to 100 % buffer B (Buffer A + 300 m*M* Imidazole) over 20 CVs collecting 1.6 mL fractions. Peak fractions containing *Tb*Arl6 were pooled and concentrated for size exclusion chromatography. The protein was applied to a 26/60 Superdex 75 column which had been equilibrated in SEC buffer (10 m*M* HEPES pH 7.0, 250 m*M* NaCl, 5 m*M* $MgCl_2$, 1 m*M* DTT). After a void volume of 80 mL, 4 mL fractions were collected. Peak fractions containing pure *Tb*Arl6 were combined and concentrated to 92 mg/mL as determined by the A_{280} using an extinction coefficient of 15470/M/cm and a molecular mass of 21803.8.

TbArl6:GppNp complex crystallisation

A stock of 200 m*M* guanosine 5′-[β,γ-imido]triphosphate (GppNp) was added to 92 mg/mL *Tb*Arl6 to give a final concentration of 8 m*M*. Crystallisation trials were set up using a Mosquito robot (TTP Labtech). Crystals were obtained in 0.2 M CsCl, 2.2 M $(NH_4)_2SO_4$ and were of sufficient quality for data collection.

X-ray data collection, processing and structure determination

Crystals were cryo-cooled to 100K by plunging directly into liquid nitrogen without the addition of cryo-protectant. Diffraction images were collected at Diamond Light Source, station I04, with a wavelength of 0.979 Å and indexed using XDS.[51] Subsequent data processing was performed using the CCP4 software package.[52] The structure was determined by molecular replacement using MrBUMP[53] which used the human Arl6 structure (PDB code 2h57) as the search model. A round of autobuilding was performed with BUCCANEER[54] to assign the sequence. Subsequent refinement and manual model building were performed using REFMAC5[55] and COOT[56] respectively. The quality of the model was monitored throughout rebuilding and refinement using MolProbity.[57] Data processing and structure refinement statistics can be found in Table I.

The X-ray data and coordinates have been deposited in the PDB with the accession code 4bas.

Size exclusion chromatography with Multi-Angle Laser Light Scattering (SEC-MALLS) analysis

Around 50 μL samples of *Tb*Arl6 at 1 and 5 mg/mL were loaded onto a BioSep-SEC-S 3000 column (Phenomenex) equilibrated in 50 m*M* HEPES pH 7.0, 5 m*M* $MgCl_2$, 250 m*M* NaCl, 1 m*M* DTT in the presence of 1 m*M* GppNp or 1 m*M* GDP. Light scattering data were recorded on a Dawn Heleos II 18-angle light scattering detector with an in-line OptilabrEX refractive index monitor (Wyatt Technology). Data were analysed using the ASTRA software and fitted to the Zimm model with an estimated d*n*/d*c* value of 0.186 mL/g.

Acknowledgments

We thank Diamond Light Source beamline IO4 for provision of X-ray data collection facilities. Funding was provided by Welcome Trust Programme Grant 077503 to DFS.

REFERENCES

1. Simarro PP, Cecchi G, Paone M, Franco JR, Diarra A, Ruiz JA, Fevre EM, Courtin F, Mattioli RC, Jannin JG (2010) The Atlas of human African trypanosomiasis: a contribution to global mapping of neglected tropical diseases. Int J Health Geogr 9:57.
2. Branche C, Kohl L, Toutirais G, Buisson J, Cosson J, Bastin P (2006) Conserved and specific functions of axoneme components in trypanosome motility. J cell sci 119:3443–3455.
3. Broadhead R, Dawe HR, Farr H, Griffiths S, Hart SR, Portman N, Shaw MK, Ginger ML, Gaskell SJ, McKean PG, Gull K (2006) Flagellar motility is

required for the viability of the bloodstream trypanosome. Nature 440:224–227.
4. Ralston KS, Hill KL (2006) Trypanin, a component of the flagellar Dynein regulatory complex, is essential in bloodstream form African trypanosomes. PLoS Pathog 2:e101.
5. Engstler M, Pfohl T, Herminghaus S, Boshart M, Wiegertjes G, Heddergott N, Overath P (2007) Hydrodynamic flow-mediated protein sorting on the cell surface of trypanosomes. Cell 131:505–515.
6. Vickerman K (1969) On the surface coat and flagellar adhesion in trypanosomes. J cell sci 5:163–193.
7. Vickerman K (1985) Developmental cycles and biology of pathogenic trypanosomes. Br Med Bull 41:105–114.
8. Hill KL (2003) Biology and mechanism of trypanosome cell motility. Eukaryot Cell 2:200–208.
9. Ginger ML, Portman N, McKean PG (2008) Swimming with protists: perception, motility and flagellum assembly. Nat Rev Microbiol 6:838–850.
10. Fliegauf M, Benzing T, Omran H (2007) When cilia go bad: cilia defects and ciliopathies. Nat Rev Mol cell biol 8:880–893.
11. Iqbal H, Wahedi HM, Hafeez FY, Mir A (2010) Molecular variants of Bardet-Biedl Syndrome. J Cell Biol Genet 1:1–11.
12. Forsythe E, Beales PL (2012) Bardet-Biedl syndrome. Eur J Hum Genet.
13. Nachury MV, Loktev AV, Zhang Q, Westlake CJ, Peranen J, Merdes A, Slusarski DC, Scheller RH, Bazan JF, Sheffield VC, Jackson PK (2007) A core complex of BBS proteins cooperates with the GTPase Rab8 to promote ciliary membrane biogenesis. Cell 129:1201–1213.
14. Loktev AV, Zhang Q, Beck JS, Searby CC, Scheetz TE, Bazan JF, Slusarski DC, Sheffield VC, Jackson PK, Nachury MV (2008) A BBSome subunit links ciliogenesis, microtubule stability, and acetylation. Dev Cell 15: 854–865.
15. Berbari NF, Lewis JS, Bishop GA, Askwith CC, Mykytyn K (2008) Bardet-Biedl syndrome proteins are required for the localization of G protein-coupled receptors to primary cilia. Proc Natl Acad Sci U S A 105: 4242–4246.
16. Domire JS, Green JA, Lee KG, Johnson AD, Askwith CC, Mykytyn K (2011) Dopamine receptor 1 localizes to neuronal cilia in a dynamic process that requires the Bardet-Biedl syndrome proteins. Cell Mol Life Sci 68: 2951–2960.
17. Wei Q, Zhang Y, Li Y, Zhang Q, Ling K, Hu J (2012) The BBSome controls IFT assembly and turnaround in cilia. Nat Cell Biol 14:950–957.
18. Jin H, White SR, Shida T, Schulz S, Aguiar M, Gygi SP, Bazan JF, Nachury MV (2010) The conserved Bardet-Biedl syndrome proteins assemble a coat that traffics membrane proteins to cilia. Cell 141:1208–1219.
19. Lu L, Horstmann H, Ng C, Hong W (2001) Regulation of Golgi structure and function by ARF-like protein 1 (Arl1). J cell sci 114:4543–4555.
20. Bhamidipati A, Lewis SA, Cowan NJ (2000) ADP ribosylation factor-like protein 2 (Arl2) regulates the interaction of tubulin-folding cofactor D with native tubulin. J Cell Biol 149:1087–1096.
21. Nakae I, Fujino T, Kobayashi T, Sasaki A, Kikko Y, Fukuyama M, Gengyo-Ando K, Mitani S, Kontani K, Katada T (2010) The arf-like GTPase Arl8 mediates delivery of endocytosed macromolecules to lysosomes in Caenorhabditis elegans. Mol Biol Cell 21:2434–2442.
22. Cevik S, Hori Y, Kaplan OI, Kida K, Toivenon T, Foley-Fisher C, Cottell D, Katada T, Kontani K, Blacque OE (2010) Joubert syndrome Arl13b functions at ciliary membranes and stabilizes protein transport in Caenorhabditis elegans. J Cell Biol 188:953–969.
23. Chiang AP, Nishimura D, Searby C, Elbedour K, Carmi R, Ferguson AL, Secrist J, Braun T, Casavant T, Stone EM, Sheffield VC (2004) Comparative genomic analysis identifies an ADP-ribosylation factor-like gene as the cause of Bardet-Biedl syndrome (BBS3). Am J Hum Genet 75:475–484.
24. Fan Y, Esmail MA, Ansley SJ, Blacque OE, Boroevich K, Ross AJ, Moore SJ, Badano JL, May-Simera H, Compton DS, Green JS, Lewis RA, van Haelst MM, Parfrey PS, Baillie DL, Beales PL, Katsanis N, Davidson WS, Leroux MR (2004) Mutations in a member of the Ras superfamily of small GTP-binding proteins causes Bardet-Biedl syndrome. Nat Genet 36:989–993.
25. Kobayashi T, Hori Y, Ueda N, Kajiho H, Muraoka S, Shima F, Kataoka T, Kontani K, Katada T (2009) Biochemical characterization of missense mutations in the Arf/Arl-family small GTPase Arl6 causing Bardet-Biedl syndrome. Biochem Biophys Res Commun 381: 439–442.
26. Zhang Q, Nishimura D, Seo S, Vogel T, Morgan DA, Searby C, Bugge K, Stone EM, Rahmouni K, Sheffield VC (2011) Bardet-Biedl syndrome 3 (Bbs3) knockout mouse model reveals common BBS-associated phenotypes and Bbs3 unique phenotypes. Proc Natl Acad Sci USA 108(51):20678–20683.
27. Ou G, Blacque OE, Snow JJ, Leroux MR, Scholey JM (2005) Functional coordination of intraflagellar transport motors. Nature 436:583–587.
28. Price HP, Hodgkinson MR, Wright MH, Tate EW, Smith BA, Carrington M, Stark M, Smith DF (2012) A role for the vesicle-associated tubulin binding protein ARL6 (BBS3) in flagellum extension in *Trypanosoma brucei*. Biochim Biophys Acta 1823:1178–1191.
29. Wittinghofer A, Vetter IR (2011) Structure-function relationships of the G domain, a canonical switch motif. Annu Rev Biochem 80:943–971.
30. Krissinel E, Henrick K (2007) Inference of macromolecular assemblies from crystalline state. J mol biol 372: 774–797.
31. Di Tommaso P, Moretti S, Xenarios I, Orobitg M, Montanyola A, Chang JM, Taly JF, Notredame C (2011) T-Coffee: a web server for the multiple sequence alignment of protein and RNA sequences using structural information and homology extension. Nucl Acids Res 39:W13–W17.
32. Ashkenazy H, Erez E, Martz E, Pupko T, Ben-Tal N (2010) ConSurf 2010: calculating evolutionary conservation in sequence and structure of proteins and nucleic acids. Nucl Acids Res 38:W529–533.
33. Dundas J, Ouyang Z, Tseng J, Binkowski A, Turpaz Y, Liang J (2006) CASTp: computed atlas of surface topography of proteins with structural and topographical mapping of functionally annotated residues. Nucl Acids Res 34:W116–118.
34. Krissinel E, Henrick K (2004) Secondary-structure matching (SSM), a new tool for fast protein structure alignment in three dimensions. Acta Crystallogr D Biol Crystallogr 60:2256–2268.
35. Wiens CJ, Tong Y, Esmail MA, Oh E, Gerdes JM, Wang J, Tempel W, Rattner JB, Katsanis N, Park H-W, Leroux MR (2010) Bardet-Biedl syndrome-associated small GTPase ARL6 (BBS3) functions at or near the ciliary gate and modulates Wnt signaling. J Biol Chem 285:16218–16230.
36. Beck R, Sun Z, Adolf F, Rutz C, Bassler J, Wild K, Sinning I, Hurt E, Brügger B, Béthune J, Wieland F (2008) Membrane curvature induced by Arf1-GTP is

essential for vesicle formation. Proc Natl Acad Sci USA 105:11731–11736.
37. Beck R, Prinz S, Diestelkötter-Bachert P, Röhling S, Adolf F, Hoehner K, Welsch S, Ronchi P, Brügger B, Briggs JAG, Wieland F (2011) Coatomer and dimeric ADP ribosylation factor 1 promote distinct steps in membrane scission. J Cell Biol 194:765–777.
38. Gasper R, Meyer S, Gotthardt K, Sirajuddin M, Wittinghofer A (2009) It takes two to tango: regulation of G proteins by dimerization. Nat Rev Mol Cell Biol 10: 423–429.
39. Vetter IR, Wittinghofer A (2001) The guanine nucleotide-binding switch in three dimensions. Science 294: 1299–1304.
40. Rodnina MV (2009) Visualizing the protein synthesis machinery: new focus on the translational GTPase elongation factor Tu. Proc Natl Acad Sci U S A 106: 969–970.
41. Der CJ, Finkel T, Cooper GM (1986) Biological and biochemical properties of human rasH genes mutated at codon 61. Cell 44:167–176.
42. Vogel US, Dixon RA, Schaber MD, Diehl RE, Marshall MS, Scolnick EM, Sigal IS, Gibbs JB (1988) Cloning of bovine GAP and its interaction with oncogenic ras p21. Nature 335:90–93.
43. Chakrabarti PP, Daumke O, Suveyzdis Y, Kotting C, Gerwert K, Wittinghofer A (2007) Insight into catalysis of a unique GTPase reaction by a combined biochemical and FTIR approach. J mol biol 367:983–995.
44. Daumke O, Weyand M, Chakrabarti PP, Vetter IR, Wittinghofer A (2004) The GTPase-activating protein Rap1GAP uses a catalytic asparagine. Nature 429: 197–201.
45. Scrima A, Thomas C, Deaconescu D, Wittinghofer A (2008) The Rap-RapGAP complex: GTP hydrolysis without catalytic glutamine and arginine residues. Embo J 27:1145–1153.
46. Cook WJ, Smith CD, Senkovich O, Holder AA, Chattopadhyay D (2010) Structure of Plasmodium falciparum ADP-ribosylation factor 1. Acta Crystallogr Sect F Struct Biol Cryst Commun 66:1426–1431.
47. Panjkovich A, Daura X (2010) Assessing the structural conservation of protein pockets to study functional and allosteric sites: implications for drug discovery. BMC Struct Biol 10:9.
48. Antonny B, Beraud-Dufour S, Chardin P, Chabre M (1997) N-terminal hydrophobic residues of the G-protein ADP-ribosylation factor-1 insert into membrane phospholipids upon GDP to GTP exchange. Biochemistry 36:4675–4684.
49. Maurer-Stroh S, Eisenhaber B, Eisenhaber F (2002) N-terminal N-myristoylation of proteins: refinement of the sequence motif and its taxon-specific differences. J mol biol 317:523–540.
50. Eisenhaber B, Bork P, Yuan Y, Loffler G, Eisenhaber F (2000) Automated annotation of GPI anchor sites: case study C. elegans. Trends Biochem Sci 25:340–341.
51. Kabsch W (2010) Xds. Acta Crystallogr D Biol Crystallogr 66:125–132.
52. Winn MD, Ballard CC, Cowtan KD, Dodson EJ, Emsley P, Evans PR, Keegan RM, Krissinel EB, Leslie AG, McCoy A, McNicholas SJ, Murshudov GN, Pannu NS, Potterton EA, Powell HR, Read RJ, Vagin A, Wilson KS (2011) Overview of the CCP4 suite and current developments. Acta Crystallogr D Biol Crystallogr 67: 235–242.
53. Keegan RM, Winn MD (2007) Automated search-model discovery and preparation for structure solution by molecular replacement. Acta Crystallogr D Biol Crystallogr 63:447–457.
54. Cowtan K (2006) The Buccaneer software for automated model building. 1. Tracing protein chains. Acta Crystallogr D Biol Crystallogr 62:1002–1011.
55. Murshudov GN, Vagin AA, Dodson EJ (1997) Refinement of macromolecular structures by the maximum-likelihood method. Acta Crystallogr D 53:240–255.
56. Emsley P, Cowtan K (2004) Coot: model-building tools for molecular graphics. Acta Crystallogr D Biol Crystallogr 60:2126–2132.
57. Davis IW, Leaver-Fay A, Chen VB, Block JN, Kapral GJ, Wang X, Murray LW, Arendall WB, 3rd, Snoeyink J, Richardson JS, Richardson DC (2007) MolProbity: all-atom contacts and structure validation for proteins and nucleic acids. Nucleic Acids Res 35:W375–W383.
58. McNicholas S, Potterton E, Wilson KS, Noble MEM (2011) Presenting your structures: the CCP4mg molecular-graphics software. Acta Crystallogr D 67:386–394.
59. Bond CS, Schuttelkopf AW (2009) ALINE: a WYSIWYG protein-sequence alignment editor for publication-quality alignments. Acta Crystallogr D Biol Crystallogr 65: 510–512.